Neutron Scattering in the Plane of Membranes: Structure of Alamethicin Pores

Ke He,* Steve J. Ludtke,* David L. Worcester,† and Huey W. Huang*
*Physics Department, Rice University, Houston, Texas 77005-1892, and †Biology Division, University of Missouri, Columbia, Missouri 65211 USA

ABSTRACT A technique of neutron in-plane scattering for studying the structures of peptide pores in membranes is described. Alamethicin in the inserted state was prepared in undeuterated and deuterated dilauroyl phosphatidylcholine (DLPC) hydrated with D_2O or H_2O. Neutron in-plane scattering showed a strong dependence on deuteration, clearly indicating that water is a part of the high-order structure of inserted alamethicin. The data are consistent with the simple barrel-stave model originally proposed by Baumann and Mueller. The theoretical curves computed with this model at four different deuteration conditions agree with the data in all cases. Both the diameter of the water pore and the effective outside diameter of the channel are determined accurately. Alamethicin forms pores in a narrow range of size. In a given sample condition, >70% of the peptide forms pores of n and $n \pm 1$ monomers. The pore size varies with hydration and with lipid. In DLPC, the pores are made of $n = 8$–9 monomers, with a water pore ~18 Å in diameter and with an effective outside diameter of ~40 Å. In diphytanoyl phosphatidylcholine, the pores are made of $n \approx 11$ monomers, with a water pore ~26 Å in diameter, with an effective outside diameter of ~50 Å.

INTRODUCTION

In previous publications (He et al., 1993a,b, 1994) we demonstrated x-ray scattering with the momentum transfer oriented in the plane of membranes detecting the lateral distribution of gramicidin channels. The principle of neutron scattering is the same as x-ray scattering. But whereas an x-ray scattering amplitude is proportional to the number of electrons an atom carries (i.e., the atomic number), a neutron scattering amplitude is determined by the nuclear property of the atom (except for magnetic materials). A particular advantage of neutron scattering is the possibility of exchanging H_2O with D_2O with little disturbance to the molecular configurations in the sample. The scattering lengths of H and D are very different. Therefore, if water is a part of the scattering object, as in the case of a membrane pore, we can vary the scattering amplitude by D_2O exchange without changing the molecular configuration of the pore. Therefore, a neutron experiment including D_2O exchange imposes a greater constraint on the theoretical analysis than does an x-ray experiment alone. In this paper we use neutron in-plane scattering to analyze the membrane pores formed by alamethicin.

Alamethicin is a 20-amino acid peptide produced by the fungus *Trichoderma viride*. Its channel-forming property has been a subject of research since the late 1960s (Mueller and Rudin, 1968). Two major components of the natural product differing by one amino acid have been identified (Pandey et al., 1977):

Alamethicin I (II):

$$\text{Ac-Aib-Pro-Aib-Ala-Aib-}\underset{(\text{Aib})}{\overset{\text{Ala}}{}}\text{-Gln-Aib-}$$

$$\text{Val-Aib-Gly-Leu-Aib-Pro-Val-Aib-Aib-Glu-Gln-Phl}$$

where the N-terminal residue is acetylated (Ac-) and the C-terminal residue is L-phenylalaninol (Phl). The peptide has eight or nine α-aminoisobutyric acid (Aib) residues. X-ray crystallography showed that alamethicin forms an α-helix with a bend at Pro 14 (Fox and Richards, 1982). Because the single channels of alamethicin fluctuate among a number of conduction levels, it was proposed originally by Baumann and Mueller (1974) that the channels are formed by alamethicin helices in a barrel-stave configuration. Each conduction level then represents a pore made of n monomers, with n varying from ~4 to 10. Indeed, the majority of the single-channel conduction experiments can be understood by using such a model (see early reviews by Latorre and Alvarez, 1981, and by Hall et al., 1984; and the most recent review by Mak and Webb, 1995).

The single channels are fluctuation phenomena. They are observed under the condition that the majority of membrane-bound alamethicin is adsorbed on the membrane surface (Huang and Wu, 1991). A very small fraction of the alamethicin is inserted in the lipid bilayer. This fraction is increased in the presence of a transmembrane electric potential because helices possess dipole moments (Baumann and Mueller, 1974). The inserted helices form transient channels with lifetimes in minutes, depending on temperature and the nature of the membrane (Mak and Webb, 1995). Within its lifetime, a channel typically fluctuates among three, four, or five conduction levels, dwelling in each level for a fraction of a second. More recently we found that at high concentrations alamethicin can be com-

Received for publication 22 November 1995 and in final form 4 March 1996.

Address reprint requests to Dr. Huey W. Huang, Department of Physics, Rice University, Houston, TX 77005-1892. Tel.: 713-527-4899; Fax: 713-527-9033; E-mail: huang@ion.rice.edu.

0006-3495/96/06/2659/08 $2.00

pletely inserted in a lipid bilayer (Huang and Wu, 1991). Here we will show by the technique of neutron in-plane scattering that alamethicin forms stable aqueous pores in the inserted state. This transition from the surface state at low concentrations to the inserted state at high concentrations is probably related to alamethicin's biological function (Ludtke et al., 1994), i.e., lysing bacterial cells (Jen et al., 1987).

Alamethicin is one of many membrane-active antibacterial peptides found in nature (see Boman et al., 1994, for a review). Many, like alamethicin, are amphipathic and adopt helical configurations when they are associated with lipid bilayers. Some of them are the major factors in the host-defense systems of animals; the best known of them are cecropins (Hultmark et al., 1980) and magainins (Zasloff, 1987). Some of them are toxins; the best known example is melittin from bee venom (Habermann, 1972). Studies of alamethicin may shed light on the molecular mechanisms of this class of peptides. Preliminary results have been published (He et al., 1995).

EXPERIMENT

Sample preparation

1,2-Dilauroyl-*sn*-glycero-3-phosphatidylcholine (DLPC) and 1,2-diphytanoyl-*sn*-glycero-3-phosphatidylcholine (DPhPC) in chloroform were purchased from Avanti Polar Lipids (Alabaster, AL). The deuterated DLPC(d46), with all the hydrogens in the carbon chains deuterated, was specially ordered from Avanti. Alamethicin was purchased from Sigma Chemical Co. (St. Louis, MO). The Sigma product (synthesized by the method of Brewer et al., 1987) is a mixture of components, principally alamethicin I (85% by high-performance liquid chromatography) and alamethicin II (12%) (Pandey et al., 1977). Both lipid and peptide were used without further purification. Deuterium oxide (D_2O, 99.9%) was purchased from Sigma. The peptide and lipid, at the desired peptide/lipid molar ratio (*P/L*), were dissolved in chloroform with several drops of methanol added to help dissolve the peptide and lipid. The solvents were removed first by a slow nitrogen purge and then in a freeze dryer under vacuum (<10 μm Hg) for ~20 h. After solvents were completely removed, D_2O or H_2O was added to the peptide/lipid mixture. The mixture was homogenized with a sonicator to break up large aggregates and then was lyophilized. The lyophilized powder was hydrated with D_2O or H_2O vapor. The samples were kept in the dark and stored at room temperature. The whole hydration process took about 2–3 weeks. Pure lipid samples were prepared in the same way. The peptide orientation in the membranes was examined by oriented circular dichroism (Wu et al., 1995). In fully hydrated DLPC, alamethicin is in the inserted phase at all concentrations we have measured: $1/10 \geq P/L \geq 1/200$. In fully hydrated DPhPC, the inserted phase occurs at $P/L \geq 1/17$, and the surface adsorption phase at $P/L \leq 1/40$; between 1/17 and 1/40 is the coexistence phase (Wu et al., 1995).

Quartz plates of 0.25-mm thickness were purchased from Chemglass (Vineland, NJ). They were cleaned with hot sulfuric and chromic acid and then thoroughly rinsed with distilled water and ethanol, until the final rinse totally wetted the surface with no water beading. The plates were dried in the oven (~300°C) and cooled to room temperature before use.

At room temperature the fully hydrated peptide/lipid mixtures were in the liquid crystalline phase (Wu et al., 1995). They were aligned into parallel multilayers between quartz plates (Asher and Pershan, 1979; Huang and Olah, 1987). Six thin layers of hydrated lipid/peptide mixture, each weighing about 6–7 mg, were held between seven parallel quartz plates. The total thickness, including the quartz plates and the sample, was ~2.0 mm. The total thickness of the samples was ~0.25 mm, and the diameter was ~15 mm. During this sample-making process, a sample could lose some of its water content through evaporation, so the aligned sample was rehydrated with D_2O or H_2O vapor for another 1–2 days before being sealed in a sample holder. The sample holder was made of aluminum with two quartz windows (0.25 mm thick).

It was possible to examine the condition of each layer of the sample under a polarized microscope. One signature of the smectic liquid crystalline phase is the presence of defect structures called oily streaks. An oily streak is paired disclinations with transverse striations, as shown schematically in the inset of Fig. 1 (Asher and Pershan, 1979; Schneider and Webb, 1984). The birefringence of the defect makes the streaks appear as bright lines between crossed polarizers (Fig. 1). Each dark area surrounded by oily streaks is a monodomain, in which the multilayers are perfectly aligned parallel to the quartz surfaces. The size of monodomains in Fig. 1 is typically 10^2 to 10^3 μm. These are the coherent regions for in-plane scattering. The key to a successful in-plane scattering experiment is to control the density of oily streaks in the sample, as will be discussed below. Techniques of controlling the smectic defects have been discussed in earlier publications (Powers and Pershan, 1977; Asher and Pershan, 1979; Huang and Olah, 1987).

Neutron in-plane scattering

For scattering angles 2θ less than 20°, the multilayer sample may be oriented normal to the incident beam. The result is indistinguishable from $\omega - 2\theta$ scan, where the momentum transfer $\mathbf{q}$ is precisely in the plane of the bilayers (He et al., 1993a). The signal of in-plane scattering in the liquid state of membranes is broad, so if $\mathbf{q}$ is slightly off the plane, the result is practically unchanged. For the same reason, the precise orientation of the sample with respect to the incident beam is not critical. The most convenient facilities for in-plane scattering experiments are small-angle scattering instruments. Our neutron in-plane scattering experiments were performed at the Intense Pulsed Neutron Source (IPNS). Argonne National Laboratory, with the Small-Angle Diffractometer (SAD). Preliminary experiments were performed at the Cold Neutron Research Facility, National Institute of Standards and Technology (NIST), with the NG-7 30-meter Small Angle Neutron Scattering Instrument, and at the University of Missouri Research Reactor.

The SAD at the IPNS is a short-flight-path time-of-flight instrument. The range of neutron wavelength is λ = 0.5–14 Å, and the momentum transfer q = 0.005–0.35 Å^{-1}. To increase the high q range to 0.5 Å^{-1}, the detector was moved off center. The beam diameter at the sample was 8 mm. The beam flux on sample (0.5–14 Å) was about 4×10^4 neutron/cm^2/s. The neutron data were collected for 5 h for each sample at room temperature.

Fig. 2 shows typical neutron in-plane scattering data. Fig. 2 *A* shows results for pure DLPC. In principle, in-plane scattering from aligned multilayers with homogeneous in-plane density should have no significant q dependence for $q \ll 2\pi$/(in-plane molecular dimension) $\approx$ 1.4 Å^{-1} (He et al., 1993b). The sharp peak at $q \approx 0.12$ Å^{-1} is the first-order diffraction peak by the oily streak defects, which represent a repeating array of bilayers perpendicular to the in-plane $\mathbf{q}$. Fig. 2 *C* is the scattering curve of the sample shown in Fig. 1, DLPC containing alamethicin at P/L = 1/10. The broad peak from $q \approx 0.05$ to 0.2 Å^{-1} is the scattering curve of alamethicin channels. In addition, a sharp diffraction peak also appears at $q \approx 0.12$ Å^{-1}, the same position as in pure lipid. This lamellar diffraction peak serves the important function of providing the repeat distance D of the multilayers and therefore providing the hydration condition of the sample in situ. Because the diffraction peak is much sharper than the scattering curve (the width ratio is about 1 to 10), it is easily removable from the latter. The in-plane scattering curve of the alamethicin pores is obtained by subtracting from the raw data the diffracting peak and the incoherent constant background (Fig. 2 *C*). However, if too many smectic defects are present in the sample, the lamellar peak can easily overwhelm the in-plane scattering signal. An example is given in Fig. 2 *B*. Thus controlling the amount of defects in the sample is essential for a good in-plane scattering measurement.

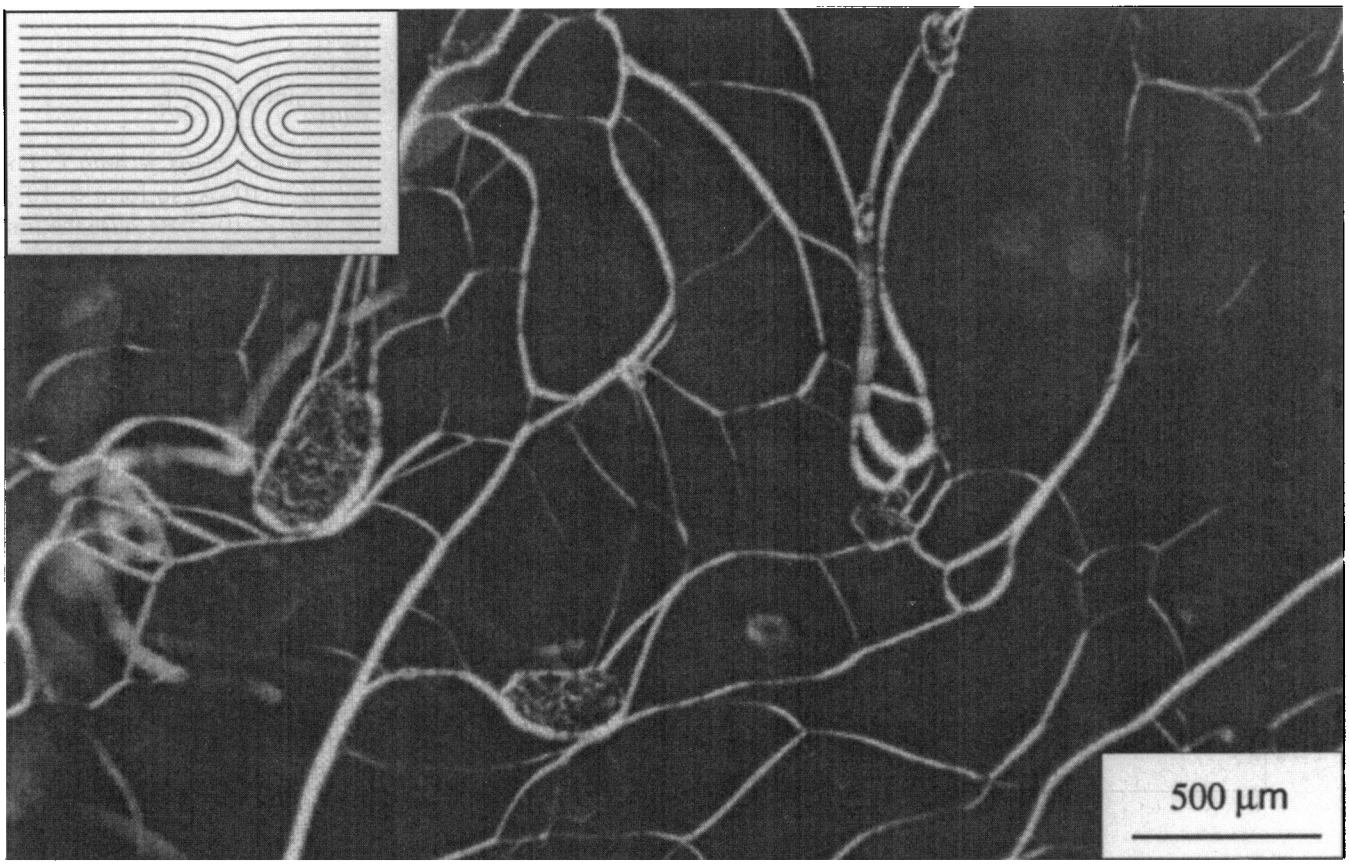

FIGURE 1 A neutron sample viewed between crossed polarizers. The microscope was focused on one of six layers. The bright lines are the smectic defects called oily streaks. The inset shows a side view of the molecular planes in an oily streak structure: the white areas are the lipid bilayers and dark lines represent the water layers (Asher and Pershan, 1979). The dark areas surrounded by the oily streaks are the aligned monodomains.

X-ray in-plane scattering

X-ray in-plane scattering was carried out as described by He et al. (1993a). Samples of pure DLPC and DLPC containing alamethicin at P/L = 1/10 were aligned between two polished, SiO_2-coated beryllium plates (0.3 mm × 10 mm diameter).

DATA ANALYSIS AND COMPUTER SIMULATION

We interpret these in-plane scattering curves with a channel model originally proposed by Baumann and Mueller (1974). We assume that the inserted alamethicin forms cylindrical channels, each made of n alamethicin helices surrounding a cylindrical water pore. The law of scattering is well established (Warren, 1969; Bacon, 1975). For in-plane scattering of objects embedded in a lipid bilayer, the scattering intensity $I(q)$ can be written as (He et al., 1993a)

$$I(q) = N \mid F(q) \mid^2 S(q), \tag{1}$$

where N is the number of channels; $F(q)$ is the scattering amplitude by an individual channel, called the form factor; and $S(q)$ is the structure factor, given by (Warren, 1969; He et al., 1993a)

$$S(q) = \frac{1}{N}\left\langle \left| \sum_j \exp(-i\mathbf{q}\cdot\mathbf{r}_j) \right|^2 \right\rangle = 1 + \int [n(r) - \bar{n}] J_0(qr) 2\pi r \mathrm{d}r + S_b(q), \tag{2}$$

where $\mathbf{r}_j$ is the position of the center of the jth channel; $n(r)2\pi r\mathrm{d}r$ is the average number of channels within the ring of radius r and width dr, centered at an arbitrarily chosen channel; $\bar{n}$ is the mean number density of channels; and $J_0(qr)$ is the zeroth order Bessel function of qr. $S_b(q)$ is the forward scattering, defined as

$$S_b(q) = \frac{1}{N}\left\langle \left| \int \frac{N}{A} \exp(-i\mathbf{q}\cdot\mathbf{r}) \mathrm{d}^2\mathbf{r} \right|^2 \right\rangle \approx \left\langle N \left(\frac{2J_1(qL)}{qL} \right)^2 \right\rangle, \tag{3}$$

where $A \approx \pi L^2$ is the area of the sample domain and the average is over the different domains. J_1 is the first-order Bessel function.

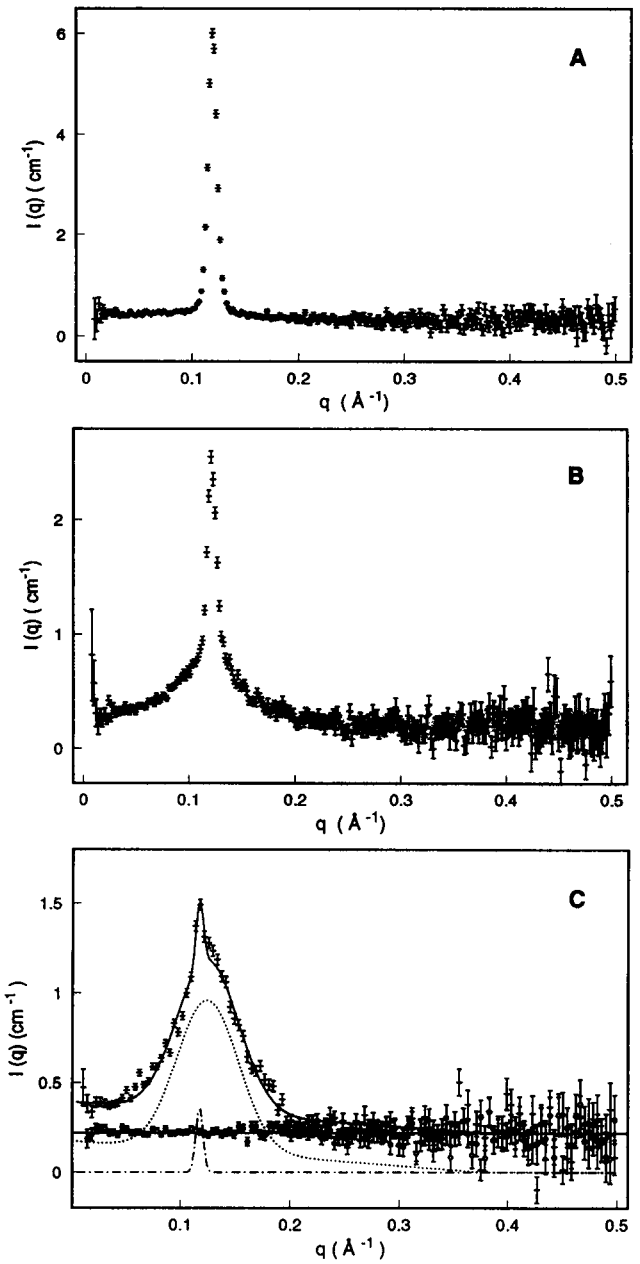

FIGURE 2 Neutron in-plane scattering of pure lipid DLPC (A) and DLPC containing alamethicin from two different preparations (B and C), all hydrated with D_2O. The smectic defects gave rise to lamellar diffraction peaks at $q \sim 0.12$ Å^{-1}. If the sample contains too many defects as in the case of (B), the diffraction peak may dominate the in-plane scattering signal; this is not desirable. The sample shown in Fig. 1 produced the data C. In this case, the lamellar peak is smaller than the in-plane scattering signal. It provided the important information of lamellar repeat distance, at the same time, it is easily removable. The raw data is decomposed into an incoherent background (straight solid line, extrapolated from the high q constant region), a gaussian fit to the diffraction peak (dash-dotted line), and the coherent scattering curve (dotted line). The diffraction peak has the same width as the peak of pure lipid (A). The recombination of these three components (solid curve) agrees well with the original data.

When $qL \gg 1$,

$$J_1(qL) \approx \sqrt{\frac{2}{\pi qL}} \sin\left(qL - \frac{\pi}{4}\right).$$

Note that $\langle \sin^2(qL) \rangle \approx 1/2$. Hence $S_b(q) = 4\bar{n}/q^3L$. For our samples, $\bar{n} \approx 10^{-3}$ Å^{-2}, $L \approx 10^6$ Å, so for $q > 10^{-2}$ Å^{-1}, the third term of Eq. 2, $S_b(q) < 10^{-2}$. Because the first and second terms of Eq. 2 are on the order of 1, the third term can be ignored. However, this term is not negligible in computer simulations.

From Eq. 2, we see that if there is a well-defined relative distance between scattering objects, one can estimate this distance from the maxima of J_0. For example, the first maximum of $J_0(qr)$ occurs at $qr = 7.016$. Our model predicts that within a channel there is a well-defined helix-helix packing distance of about 11 Å (the diameter of alamethicin). Therefore, we expect to see a maximum in the intensity at $q \approx 7.016/11 \approx 0.65$ Å^{-1}. X-ray in-plane scattering of alamethicin in DLPC at $P/L = 1/10$ (Fig. 3) indeed shows a peak at this expected position.

Computer simulation of structure factor

We compute the structure factor by simulation. We assume that the channels diffuse randomly in the plane of the bilayer, with the constraint that no two channels are allowed to overlap. From the crystallographic data (Fox and Richards, 1982), we know that an alamethicin monomer is approximately a cylinder 32 Å long and 11 Å in diameter. From the model we can calculate the outside diameter R of a channel of n monomers. The density of the channels can be calculated from the cross-sectional areas of the channel and the lipid, and the peptide lipid molar ratio P/L. The cross section of DLPC containing alamethicin at $P/L \approx 1/10$

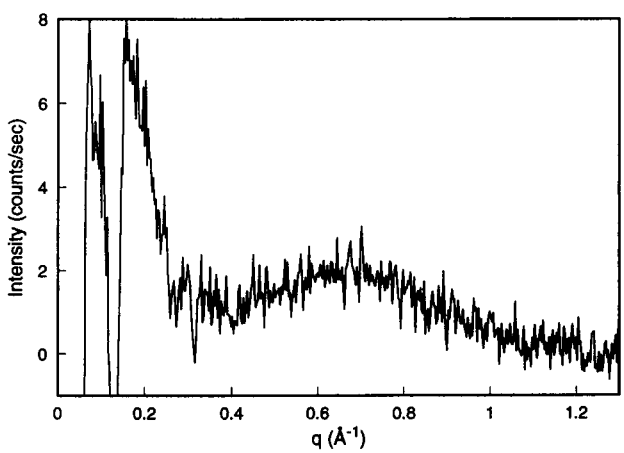

FIGURE 3 X-ray in-plane scattering of DLPC containing alamethicin at P/L = 1/10. The background of pure DLPC has been removed. The sharp peaks at $q \sim 0.1$ Å^{-1} and 0.2 Å^{-1} are the 1st and 2nd order lamellar peaks due to smectic defects. The in-plane scattering maximum at $q \sim 0.65$ Å^{-1} indicates that there is a well defined distance between scattering objects at ~7.016/0.65 = 11 Å.

is estimated from the x-ray diffraction of bilayers containing gramicidin at $P/L = 1/10$ (Olah et al., 1991) to be ~52 Å^2. For DPhPC containing alamethicin at $P/L = 1/10$, we use the phosphate-to-phosphate distance from x-ray diffraction (~36 Å; He et al., manuscript in preparation), the estimated phosphorus to chain distance (~4 Å; Wu et al., 1995; Ludtke et al., 1995), and the chain volume (~1230 Å^3; Wu et al., 1995) to estimate its cross section, ~90 Å^2.

For each alamethicin lipid ratio P/L, simulations were carried out for channels of various size n. We let 1000 channels randomly diffuse in a square plane of appropriate area with periodic boundary conditions. After the system reached equilibrium,

$$S(q) = \frac{1}{N}\left\langle \left| \sum_j \exp(-i\mathbf{q}\cdot\mathbf{r}_j) \right|^2 \right\rangle$$

was calculated and averaged over time. The forward scattering term $S_b(q)$ in Eq. 2 is negligible in experiments, but not in simulations. For a square plane of side L,

$$S_b(\mathbf{q}) = \frac{N}{L^2}\left| \int_0^L \exp(-iqx)dx \right|^2 = \frac{2N}{q^2L^2} = \frac{2\bar{n}}{q^2}. \quad (4)$$

This term can also be simulated exactly like $S(q)$, except here the channels are allowed to pass through each other with no hard-core exclusion. The simulated $S_b(q)$ is in exact agreement with the theoretical curve (Fig. 4). $S_b(q)$ is subtracted from the raw data of the $S(q)$ simulation.

In a previous study on in-plane scattering (He et al., 1993b), we have shown that the peak position of the structure factor is largely determined by the radius R and is relatively insensitive to the density of the scattering object. On the other hand, the peak width and peak amplitude are mainly determined by the density: the greater the density, the narrower the width and the larger the amplitude.

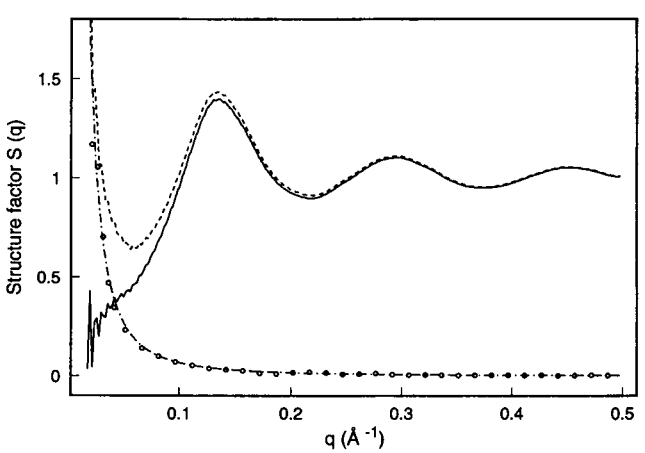

FIGURE 4 Simulated structure factor $S(q)$ (solid line) for channels of 8 monomers. It is obtained from the simulation data (dashed line) minus the forward scattering $S_b(q)$. The dash-dotted line is the theoretical expression Eq. (4). The circles are the simulated $S_b(q)$.

Form factor

The form factor of an alamethicin channel is given by (He et al., 1993b)

$$F(\mathbf{q}) = \int_0^r \rho_{pore}(\mathbf{r}) \exp[-i\mathbf{q}\cdot(\mathbf{r}-\mathbf{r}_p)]d^3\mathbf{r} + \int_r^R \rho_{ala}(\mathbf{r}) \exp[-i\mathbf{q}\cdot(\mathbf{r}-\mathbf{r}_q)]d^3\mathbf{r}. \quad (5)$$

The channel has a distinct region of water pore of radius r and an alamethicin ring of outside radius R. For $q \ll 2\pi/$(in-plane molecular dimension), the molecules are considered uniformly distributed in each region. ρ represents the scattering length density contrast of each region relative to the lipid background. The latter is also treated as a uniform region. With this approximation, Eq. 5 can be integrated:

$$F(q) = 2\rho_{pore}V_{pore}\frac{J_1(qr)}{qr} + 2\rho_{ring}V_{ring}\frac{RJ_1(qR) - rJ_1(qr)}{q(R^2 - r^2)}, \quad (6)$$

where V_{pore} and V_{ring} are the volumes of the pore region and ring region, respectively.

The neutron scattering length densities of alamethicin, DLPC, and water are calculated and shown in Table 1. Alamethicin has 15 hydrogen bonds in its α-helical conformation (Fox and Richards, 1982). When the samples are hydrated with D_2O, 15 exchangeable hydrogens in its backbone are replaced by deuterium. Therefore, the scattering length density of alamethicin is increased from 1.82×10^{10} cm^{-2} to 2.52×10^{10} cm^{-2}. An example of form factor is shown in the following.

Consider a channel formed by eight alamethicin helices. The alamethicin helix is approximated by a cylinder 11 Å in diameter. Then the water pore radius is about 9 Å and the outside radius is about 20 Å. The crystal structure of alamethicin contained 33% organic solvent (Fox and Richards, 1982). Therefore, the peptide only occupies 66 Å^2 in cross section. As a result, the eight alamethicin monomers only occupy about 50% of the volume between radius 9 Å and radius 20 Å. We assume that the other 50% of the space is

TABLE 1 Average neutron scattering length densities (in 10^{10} cm^{-2})

	Alamethicin	Water	DLPC chain	DLPC lipid
Undeuterated	1.82	−0.562	−0.397	0.346
Deuterated	2.52*	6.35	6.99	4.80†

*Fifteen exchangeable hydrogen atoms in the alamethicin backbone were replaced by deuterium atoms.
†Only the chains are deuterated.

filled by the hydrocarbon chains of the lipid. We believe that this is reasonable because the surface of alamethicin is practically all hydrophobic, except for a narrow polar strip parallel to the helical axis consisting of Gln-7, Glu-18, and carbonyl oxygens of Aib-10 and Gly-11 (Fox and Richards, 1982). The polar strip is supposed to face the water pore. The scattering length density contrasts of the ring region and the pore region relative to the lipid background are given in Table 2. Fig. 5 shows the calculated form factor of the eight-monomer channel and the separate contributions by the pore region and the ring region. Notice that the contribution of the ring region is very small in the range of q where the scattering was observed.

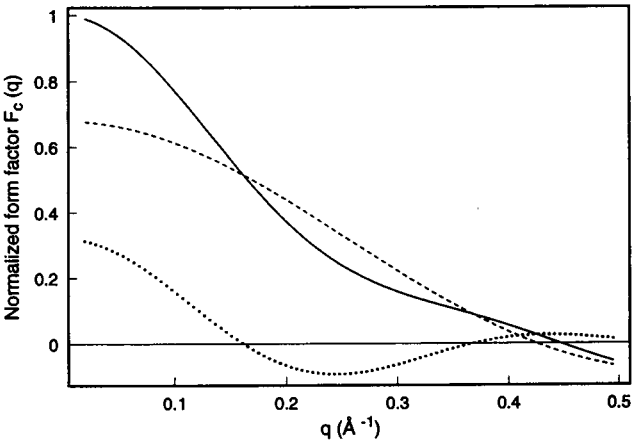

FIGURE 5 Normalized form factor $F(q)$ for a channel of 8 monomers based on the barrel-stave model. It is the sum of the form factors of the D_2O pore (dashed line) and of the surrounding alamethicin ring (dotted line). The lipid background is of undeuterated DLPC.

Structure of alamethicin pores

A stringent test of this simple model is provided by the measurements of alamethicin in DLPC in four different deuteration conditions: alamethicin in undeuterated and in deuterated DLPC, each hydrated by H_2O or D_2O. Four form factors are calculated for the same pore configuration at these deuterations. With the same structure factor, $|F(q)|^2 S(q)$ are compared with four sets of neutron in-plane scattering data. In Figs. 6 and 7, we show that the theoretical curves of eight-monomer channels fit all four sets of data quite well. The sensitivity of the model can be seen by a comparison of three different sizes of channel: $n = 7, 8, 9$ (Fig. 8). Clearly, $n = 7$ and 9 deviate from the data substantially. However, the data could not differentiate the monodispersion of eight-monomer channels from a Gaussian distribution of sizes centered at eight monomers as long as the width of the distribution is sufficiently narrow, for example, >70% of the channels are $n = 7$, 8, and 9. Thus we conclude that inserted alamethicin forms pores in a narrow range of size. Most of them (>70%) are made of n and $n \pm 1$ monomers. In comparison, the single channels observed at low peptide concentrations often fluctuate among four or five different conduction levels (Latorre and Alvarez, 1981; Mak and Webb, 1995). As mentioned above, the peak width and the peak amplitude of the structure factor are sensitive to the density of the scattering object. The neutron data are consistent with the assumption that all of the inserted alamethicin is involved in pore formation.

The most sensitive parameter resulting from this analysis is the size of the water pore. Because the neutron contrast of peptide against lipid is much smaller than D_2O against CH_2 or H_2O against CD_2, the most sensitive parameter for the form factor is the radius of the water pore. Qualitatively speaking, the high q side of the scattering curve determines the form factor, which in this case determines the size of the water pore. On the other hand, the low q side of the scattering curve is largely determined by the structure factor. As mentioned above, the peak position of the structure factor is most sensitive to the outside radius R. Therefore, this analysis determines both r and R quite accurately (±1 Å). However, we have to regard R as an effective outside radius, because in our model we have neglected the possibility of interactive potentials (besides the hard-core repulsion) between channels, which would have affected the structure factor. For example, if there is an attractive potential between channels, the effective outside radius would appear to be smaller than the physical radius. Channel-

TABLE 2 Neutron scattering length contrast densities (in 10^{10} cm^{-2})

Lipid/ hydration	DLPC/D_2O	DLPC/H_2O	DLPC(d46)/D_2O	DLPC(d46)/H_2O
Pore	6.0	−0.91	1.6	−5.4
Ring	0.72	0.37	−0.05	−0.40

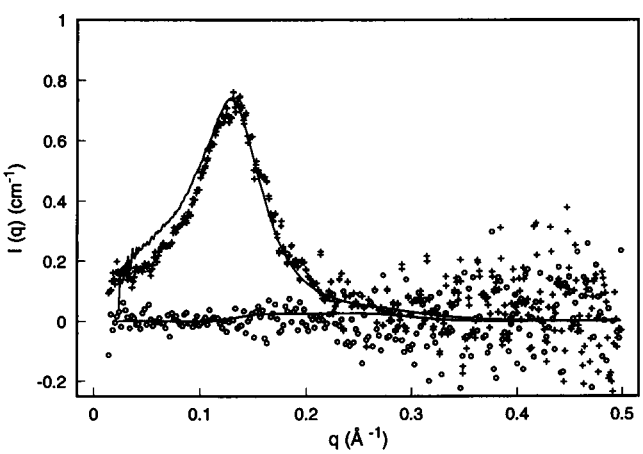

FIGURE 6 Neutron in-plane scattering curve of alamethicin pores in DLPC bilayers at P/L = 1/10 hydrated with D_2O (data +, the diffraction peak and the incoherent back ground removed-see Fig. 2). After the sample was exposed to H_2O vapor for 48 hours, the neutron scattering was not distinguishable from the constant incoherent background (data o). The lamellar spacing was ~51 Å. The solid lines are the theoretical curves of 8-monomer channels in D_2O and in H_2O.

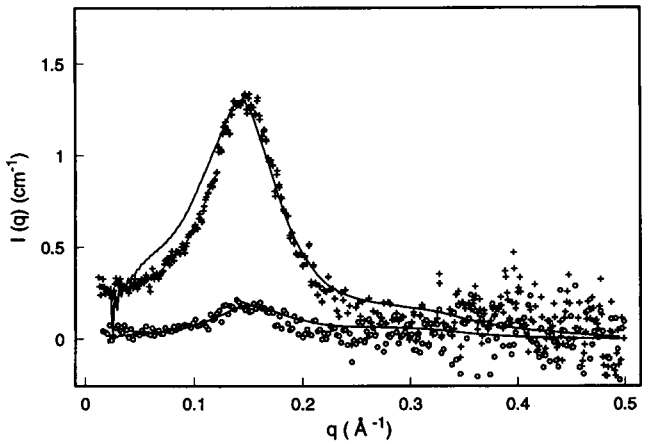

FIGURE 7 The sample conditions are the same as Fig. 6 except that the lipid is DLPC with fully deuterated chains. Data (+) and (o) are the scattering curves when the sample was hydrated with H_2O and with D_2O, respectively. The lamellar spacing was ~49 Å in both cases. The solid curves are the theoretical curves of the same model as in Fig. 6 calculated for the corresponding deuteration conditions.

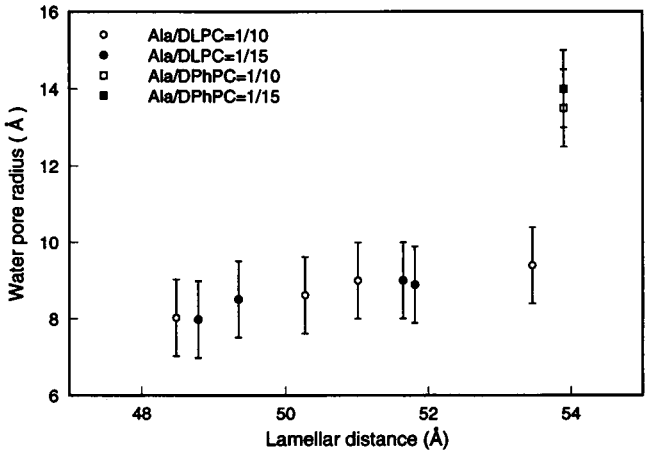

FIGURE 9 Pore size vs. lamellar repeat distance for alamethicin in DLPC and DPhPC. The error bars represent the maximum uncertainties (±1 Å) in pore radius from the data analysis.

channel interactions would also sharpen the peaks of the structure factor. We note that in Figs. 6 and 7 the data are slightly narrower than the theoretical curves on the high q side. This probably implies the existence of some membrane-mediated channel-channel interactions (e.g., Huang, 1986). Nevertheless, the simple barrel-stave model ignoring the possible interactive potentials seems to fit the data quite well.

In this experiment, it was difficult to control the water content in the samples. Fortunately, the lamellar diffraction peak due to the smectic defects in the sample provided the in situ lamellar repeat distance. We found a strong correlation between the lamellar spacing and the position of the scattering curve, implying the higher the water content, the larger the pore. Fig. 9 shows the pore size versus the lamellar repeat distance for alamethicin in DLPC at P/L = 1/10 and 1/15. Surprisingly, the pore size is rather independent of the peptide concentration. However, the pore size does vary with lipid. In DPhPC the alamethicin pores are consistently larger (He et al., 1995). These pores are formed by about 11 monomers with a water pore about 26 Å in diameter and an outside diameter about 50 Å (Fig. 9).

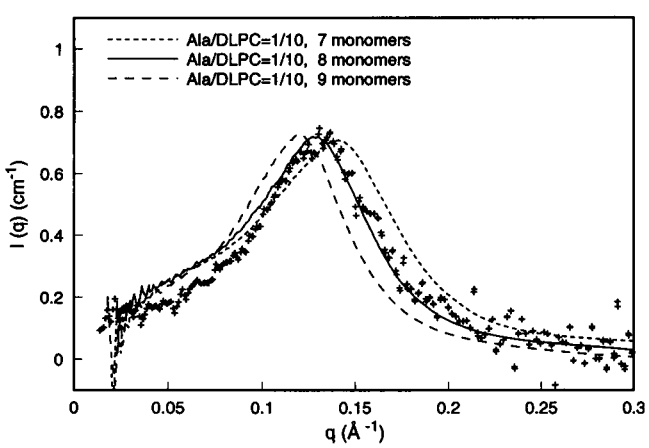

FIGURE 8 The data and the theoretical curve of Fig. 6 (+) are compared with theoretical curves of 7- and 9-monomer channels.

We thank B. Hammouda for help with experiments at NIST and thank P. Thiyagarajan and D. G. Wozniak for help with experiments at IPNS.

This work was supported in part by National Institutes of Health grant AI34367 and Biophysics Training grant GM08280; by Department of Energy grant DE-FG03-93ER61565; and by the Robert A. Welch Foundation. The facility at NIST is supported by the National Science Foundation under agreement DMR-9423101. The facility at the IPNS is funded by the Department of Energy, BES-Materials Science, under contract W-31-109-Eng-38. Use of Rice University Intel iPSC/860 for simulations was provided by the Center for Research on Parallel Computation under NSF Cooperative Agreements CCR-8809615 and CDA-8619893 with support from the Keck Foundation.

REFERENCES

Asher, S. A., and P. S. Pershan. 1979. Alignment and defect structures in oriented phosphatidycholine multilayer. *Biophys. J.* 27:393–422.

Bacon, G. E. 1975. *Neutron Diffraction,* 3rd ed. Clarendon Press, Oxford. Chap. 16. 544–580.

Baumann, G., and P. Mueller. 1974. A molecular model of membrane excitability. *J. Supramol. Struct.* 2:538–557.

Boman, H. G., J. Marsh, and J. A. Goode. 1994. Antimicrobial Peptides, Ciba Foundation Symposium. John Wiley and Sons, Chichester. 1–272.

Brewer, D., F. G. Mason, and A. Taylor. 1987. The production of alamethicin by *Trichoderma* spp. *Can. J. Microbiol.* 33:619–625.

Fox, R. O., and F. M. Richards. 1982. A voltage-gated ion channel model inferred from the crystal structure of alamethicin at 1.5-Å resolution. *Nature.* 300:325–330.

Habermann, E. 1972. Bee and wasp venoms. *Science.* 177:314–322.

Hall, J. E., I. Vodyanov, J. M. Balasubramanina, and G. R. Marshall. 1984. Alamethicin: a rich model for channel behavior. *Biophys. J.* 45:233–247.

He, K., S. J. Ludtke, D. L. Worcester, and H. W. Huang. 1995. Antimicrobial peptide pores in membranes detected by neutron in-plane scattering. *Biochemistry.* 34:15614–15618.

He, K., S. J. Ludtke, Y. Wu, and H. W. Huang. 1993a. X-ray scattering in the plane of membrane. *J. Phys. France IV.* 3:265–270.

He, K., S. J. Ludtke, Y. Wu, and H. W. Huang. 1993b. X-ray scattering with momentum transfer in the plane of membrane. Application to gramicidin organization. *Biophys. J.* 64:157–162.

He, K., S. J. Ludtke, Y. Wu, H. W. Huang, O. S. Andersen, D. Greathouse, and R. E. Koeppe. 1994. Closed state of gramicidin channel detected by x-ray in-plane scattering. *Biophys. Chem.* 49:83–89.

Huang, H. W. 1986. Deformation free energy of bilayer membrane and its effect on gramicidin channel lifetime. *Biophys. J.* 50:1061–1070.

Huang, H. W., and G. A. Olah. 1987. Uniformly oriented gramicidin channels embedded in thick monodomain lecithin multilayers. *Biophys. J.* 51:989–992.

Huang, H. W., and Y. Wu. 1991. Lipid-alamethicin interactions influence alamethicin orientation. *Biophys. J.* 60:1079–1087.

Hultmark, D., H. Steiner, T. Rasmuson, and H. G. Bowman. 1980. Insect immunity: purification and properties of three inducible bactericidal proteins from hemolymph of immunized pupae of *Hyalophora cecropia. Eur. J. Biochem.* 106:7–16.

Jen, W.-C., G. A. Jones, D. Brewer, V. O. Parkinson, and A. Taylor. 1987. The antibacterial activity of alamethicin and zervamicins. *J. Appl. Bacteriol.* 63:293–298.

Latorre, R., and S. Alvarez. 1981. Voltage-dependent channels in planar lipid bilayer membranes. *Physiol. Rev.* 61:77–150.

Ludtke, S. J., K. He, and H. W. Huang. 1995. Membrane thinning by magainin 2. *Biochemistry.* 34:16764–16769.

Ludtke, S. J., K. He, Y. Wu, and H. W. Huang. 1994. Cooperative membrane insertion of magainin correlated with its cytolytic activity. *Biochim. Biophys. Acta.* 1190:181–184.

Mak, D. D., and W. W. Webb. 1995. Two classes of alamethicin transmembrane channels: molecular models form single-channel properties. *Biophys. J.* 69:2323–2336.

Mueller, P., and D. O. Rudin. 1968. Action potentials induced in biomolecular lipid membranes. *Nature.* 217:713–719.

Pandey, R. C., J. C. Cook, and K. L. Rinehart. 1977. High resolution and field desorption mass spectrometry studies and revised structure of alamethicin i and ii. *J. Am. Chem. Soc.* 99:8469–8483.

Powers, L., and P. S. Pershan. 1977. Monodomain samples dipalmitoylphosphatidylcholine with varying concentrations of water and other ingredients. *Biophys. J.* 20:137–152.

Schneider, M. B., and W. W. Webb. 1984. Undulating paired disclinations (oily streaks) in lyotropic liquid crystals. *J. Phys. France.* 45:273–281.

Warren, B. E. 1969. X-Ray Diffraction. Dover Publications, Mineola, NY. 116–150.

Wu, Y., K. He, S. J. Ludtke, and H. W. Huang. 1995. X-ray diffraction study of lipid bilayer membranes interacting with amphiph lic helical peptides: diphytanoyl phosphatidylcholine with alamethicin at low concentration. *Biophys. J.* 68:2361–2369.

Zasloff, M. 1987. Magainins, a class of antimicrobial peptides form xenopus skin: isolation, characterization of two active forms and partial cDNA sequence of a precursor. *Proc. Natl. Acad. Sci. USA.* 84: 5449–5453.